



UNIVERSITY  
OF WOLLONGONG  
AUSTRALIA

University of Wollongong  
Research Online

---

Faculty of Engineering and Information Sciences -  
Papers: Part A

Faculty of Engineering and Information Sciences

---

2015

# Fractional order modelling of the cumulative deformation of granular soils under cyclic loading

Yifei Sun

*University of Wollongong, ys910@uowmail.edu.au*

Yang Xiao

*Chongqing University, hhxyanson@163.com*

Khairul Fikry Hanif

*University of Western Australia*

---

## Publication Details

Sun, Y., Xiao, Y. & Hanif, K. Fikry. (2015). Fractional order modelling of the cumulative deformation of granular soils under cyclic loading. *Acta Mechanica Solida Sinica*, 28 (6), 647-658.

Research Online is the open access institutional repository for the University of Wollongong. For further information contact the UOW Library:  
research-pubs@uow.edu.au

---

# Fractional order modelling of the cumulative deformation of granular soils under cyclic loading

## **Abstract**

To model the cumulative deformation of granular soils under cyclic loading, a mathematical model was proposed. The power law connection between the shear strain and loading cycle was represented by using fractional derivative approach. The volumetric strain was characterized by a modified cyclic flow rule which considered the effect of particle breakage. All model parameters were obtained by the cyclic and static triaxial tests. Predictions of the test results were provided to validate the proposed model. Comparison with an existing cumulative model was also made to show the advantage of the proposed model.

## **Disciplines**

Engineering | Science and Technology Studies

## **Publication Details**

Sun, Y., Xiao, Y. & Hanif, K. Fikry. (2015). Fractional order modelling of the cumulative deformation of granular soils under cyclic loading. *Acta Mechanica Solida Sinica*, 28 (6), 647-658.

# FRACTIONAL ORDER MODELLING OF THE CUMULATIVE DEFORMATION OF GRANULAR SOILS UNDER CYCLIC LOADING

Yifei Sun<sup>1</sup>, Yang Xiao<sup>2</sup>, Khairul Fikry Hanif<sup>3</sup>

1. Institute for Mathematics and its Applications, University of Wollongong, Wollongong 2522, Australia

2. College of Civil Engineering, Chongqing University, Chongqing 400045, China

2. Faculty of Engineering, Computing and Mathematics, University of Western Australia, Perth 6907, Australia

**ABSTRACT:** To model the cumulative deformation of granular soils under cyclic loading, a mathematical model is proposed. The power law connection between the shear strain and loading cycle is represented by using fractional derivative approach. The volumetric strain is characterized by a modified cyclic flow rule which considers the effect of particle breakage. All model parameters can be obtained by the cyclic and static triaxial tests. Predictions of the test results are provided to validate the proposed model. Comparison with an existing cumulative model is also performed to show the advantage of the proposed model.

**KEY WORDS:** cumulative deformation; cyclic stress; cyclic flow rule; fractional derivative; granular soil

## I. INTRODUCTION

Well-constructed infrastructure could still suffer differential foundation settlements and structural damages if they were exposed to continuous cyclic loadings induced by traffics, construction activities and even sea waves, etc. If the number of loading cycles is sufficiently large then even relatively small strain amplitudes may endanger the serviceability of structures in the long run, especially if their displacement tolerance is small. Miura et al. [1] reported that the additional monitoring settlement of Saga airport road resulted from landing and taking off of aircraft reached about 150 mm in just 2 years. In addition, the tunnel settlement of the Shanghai Metro Line 1 caused by dynamic train loading had reached up to 155 mm in only 4 years [2]. Detailed understanding of the cumulative deformation and failure mechanism of soils under repeated loading with large number of cycles is thus essential for the proper design and maintenance of airport roads, railway tracks and highway pavements, etc. To investigate and constitutive modeling of the cyclic stress strain response of soils, lots of experimental and theoretical studies have been conducted [3-15]. Khalili et al. [7] and Liu et al. [12] studied the cyclic behaviour of gravelly soil under cyclic loading with low frequency. Ishikawa et al. [16] examined the mechanical response of railroad ballast subjected to repeated train passages on ballasted track by using multi-ring shear test. Suiker et al. [17] and Indraratna et al. [18-20] investigated the cyclic behaviour of both ballast and subballast under low and high loading frequency, from which the influences of loading history and confining pressure as well as the loading frequency were observed. These excellent works provide fundamental tools for further understanding the cyclic behaviour of granular soils, which is significant in practical design methods for the stability of both over-

40 ground and underground structures. However, some of the tests only covered a cyclic load  
41 with very small loading cycles, say less than 100. The corresponding constitutive models,  
42 such as the bounding surface model [7, 21] and the generalized plasticity model [22-23] can  
43 only simulate the cyclic behaviour of granular soils for very limited cycles. For the  
44 cumulative strain under high loading cycles ( $N > 10^3$ ), these models usually failed due to the  
45 unintentional accumulation of numerical errors and the huge calculation effort, especially in  
46 the finite element analysis. It is of little possibility for these theoretical models to be used in  
47 practical engineering where the loads usually have at least tens of thousands of cycles. To  
48 overcome this limitation, lots of empirical and semi-empirical models were proposed. For  
49 example, Indraratna et al. [24] proposed a pressure-dependent elastoplastic model by  
50 introducing empirical parameters to consider the effect of stress history, stress ratio, number  
51 of cycles, and breakage. In fact, the cumulative deformation of granular soils under cyclic  
52 stress is not only influenced by the current loading stress but also affected by previous  
53 loading cycles. It is indeed a memory-intensive phenomenon which can be mathematically  
54 expressed by a simple power law of the loading cycles,  $N$ , as suggested by Chrismer and  
55 Selig [25] and Indraratna et al. [26], etc. Inspired by the creep of soils under constant static  
56 stress, lots of empirical models for predicting cumulative deformation of granular soils, such  
57 as sand, ballast and subballast, etc., subjected to averaged cyclic deviator stress were  
58 suggested [5-6, 8-11]. Due to the explicit expressions, these models can be easily  
59 incorporated in the engineering-oriented finite element method. However, most of the  
60 existing models contain a lot of model parameters and even so still cannot well predict the  
61 accumulation of residual strain in soils subjected to cyclic loading with many cycles. Most  
62 importantly, they did not physically explain the reason for the cumulative deformation of  
63 granular soils evolving in a power law. Sun et al. [27-28] suggested the use of fractional  
64 calculus in modeling the dependency of power law in complex mechanical process. Later,  
65 Yin et al. [29-30] proposed a framework for constitutive modeling the strain hardening and  
66 softening of geomaterials under static loading by employing the basic theory of fractional  
67 derivative. However, fractional order constitutive modeling of cumulative behaviour of soils  
68 under cyclic loading is still rarely reached. The aim of this paper is to make an attempt to  
69 model the cumulative shear strain of granular soils subjected to drained cyclic loading based  
70 on the theory of fractional derivative. Moreover, a modified cyclic flow rule considering the  
71 effect of particle breakage is proposed for determining the corresponding cumulative  
72 volumetric strain. Comparison between the experimental results and model predictions is also  
73 presented.

74

## 75 II. CUMULATIVE STRAIN BASED ON FRACTIONAL CALCULUS

### 76 2.1. General formula

77 To quantify the cyclic behaviour of granular soils, laboratory tests, including the biaxial and  
78 triaxial tests are usually conducted under either constant stress rate ( $d\sigma$ ) or constant strain  
79 rate ( $d\varepsilon$ ). By regarding the soil as an intermediate material, lying between the ideal solids

80 which obey Hooke' law and the Newtonian fluids which satisfy Newton's law of viscosity,  
 81 the stress ( $\sigma$ ) and strain ( $\varepsilon$ ) relationship should obey [29]

$$82 \quad \sigma(t) = G \frac{d^\alpha \varepsilon(t)}{dt^\alpha} \quad (1)$$

83 where  $\alpha$  denotes the fractional derivative order, ranging between 0 and 1. With  $\alpha$   
 84 approaching 1, the material behaves increasingly like an ideal solid, whereas it becomes  
 85 increasingly softer like a fluid with  $\alpha$  approaching 0.  $G$  is a material constant.  $t$  denotes the  
 86 time for loading and unloading. To start with, the Riemann-Liouville definitions of the  
 87 fractional order derivative (Eq. (2)) and integral (Eq. (3)) of function  $f$  are used [30]:

$$88 \quad \frac{d^\alpha f}{dt^\alpha} = \frac{1}{\Gamma(1-\alpha)} \frac{d}{dt} \int_0^t \frac{f(\tau)}{(t-\tau)^\alpha} d\tau \quad (2)$$

$$89 \quad \frac{d^{-\alpha} f}{dt^{-\alpha}} = \frac{1}{\Gamma(\alpha)} \int_0^t \frac{f(\tau)}{(t-\tau)^{1-\alpha}} d\tau \quad (3)$$

90 where  $\Gamma(\bullet)$  denotes the gamma function and can be formulated as

$$91 \quad \Gamma(t) = \int_0^\infty e^{-\tau} \tau^{t-1} d\tau \quad (4)$$

92 For soils loaded and then unloaded for  $N$  cycles, the total strain can be obtained by  
 93 summing the strain of each loading and unloading cycle, that is

$$94 \quad \begin{aligned} \varepsilon(t) = & \frac{1}{G_1} \frac{1}{\Gamma(\alpha)} \int_0^T \frac{\sigma(\tau)}{(t-\tau)^{1-\alpha}} d\tau + \frac{1}{G'_1} \frac{1}{\Gamma(\alpha)} \int_{\frac{T}{2}}^T \frac{\hat{\sigma}(\tau)}{(t-\tau)^{1-\alpha}} d\tau \\ & + \frac{1}{G_2} \frac{1}{\Gamma(\alpha)} \int_T^{T+\frac{T}{2}} \frac{\sigma(\tau)}{(t-\tau)^{1-\alpha}} d\tau + \frac{1}{G'_2} \frac{1}{\Gamma(\alpha)} \int_{T+\frac{T}{2}}^{2T} \frac{\hat{\sigma}(\tau)}{(t-\tau)^{1-\alpha}} d\tau \\ & + \dots + \frac{1}{G_N} \frac{1}{\Gamma(\alpha)} \int_{(N-1)T}^{(N-1)T+\frac{T}{2}} \frac{\sigma(\tau)}{(t-\tau)^{1-\alpha}} d\tau + \frac{1}{G'_N} \frac{1}{\Gamma(\alpha)} \int_{(N-1)T+\frac{T}{2}}^{NT} \frac{\hat{\sigma}(\tau)}{(t-\tau)^{1-\alpha}} d\tau \end{aligned} \quad (5)$$

95 where the time,  $T$ , denote the loading period for one complete loading and unloading process.  
 96  $\sigma$  and  $\hat{\sigma}$  denote the loading and unloading stresses, respectively.  $G_i$  and  $G'_i$  ( $i = 1, 2, 3, \dots,$   
 97  $N$ ) are the loading and unloading moduli, respectively. Rearranging Eq. (5), one has

$$98 \quad \varepsilon(t) = \sum_{i=1}^N \frac{1}{G_i} \frac{1}{\Gamma(\alpha)} \int_{(i-1)T}^{(i-1)T+\frac{T}{2}} \frac{\sigma(\tau)}{(t-\tau)^{1-\alpha}} d\tau + \sum_{i=1}^N \frac{1}{G'_i} \frac{1}{\Gamma(\alpha)} \int_{(i-1)T+\frac{T}{2}}^{iT} \frac{\hat{\sigma}(\tau)}{(t-\tau)^{1-\alpha}} d\tau \quad (6)$$

99 Following Yin et al. [29], for soils tested under triaxial loading condition, the shear strain  
 100  $\varepsilon_s$  and volumetric strain can be reformulated by using Eq. (6) as

$$101 \quad \varepsilon_s = \sum_{i=1}^N \frac{1}{G_i} \frac{1}{\Gamma(\alpha)} \int_{(i-1)T}^{(i-1)T+\frac{T}{2}} \frac{q(\tau)}{(t-\tau)^{1-\alpha}} d\tau + \sum_{i=1}^N \frac{1}{G'_i} \frac{1}{\Gamma(\alpha)} \int_{(i-1)T+\frac{T}{2}}^{iT} \frac{\hat{q}(\tau)}{(t-\tau)^{1-\alpha}} d\tau \quad (7a)$$

$$\varepsilon_v = \sum_{i=1}^N \frac{1}{K_i} \frac{1}{\Gamma(\alpha)} \int_{(i-1)T}^{(i-1)T+\frac{T}{2}} \frac{p'(\tau)}{(t-\tau)^{1-\alpha}} d\tau + \sum_{i=1}^N \frac{1}{K'_i} \frac{1}{\Gamma(\alpha)} \int_{(i-1)T+\frac{T}{2}}^{iT} \frac{\hat{p}'(\tau)}{(t-\tau)^{1-\alpha}} d\tau \quad (7a)$$

where  $\varepsilon_s = 2/3(\varepsilon_1 - \varepsilon_3)$  and  $\varepsilon_v = (\varepsilon_1 + 2\varepsilon_3)$ ;  $\varepsilon_1$  and  $\varepsilon_3$  are the first and third principal strains, respectively.  $q$  ( $=\sigma'_1 - \sigma'_3$ ) and  $p'$  ( $=\sigma'_1 + 2\sigma'_3$ )/3 are the loading deviator and mean effective principal stresses, respectively;  $\sigma'_1$  and  $\sigma'_3$  are the first and third effective principal stresses, respectively.  $\hat{q}$  denote the unloading deviator stresses.  $K_i$  and  $K'_i$  ( $i = 1, 2, 3, \dots, N$ ) are the volumetric loading and unloading moduli, respectively. Note that  $dq = d\sigma'_1$  and  $dp' = d\sigma'_1/3$  during loading and  $d\hat{q} = -d\sigma'_1$  and  $d\hat{p}' = -d\sigma'_1/3$  during unloading.

## 2.2 Formula for long-term deformation

It is noted that Eq. (6) strictly counts the strain variation of each individual loading cycle. The entire iteration steps may cause huge calculation effort and numerical errors if large amounts of loading cycles are involved. Therefore, a modified fractional order model for long-term cyclic loading needs to be proposed. As adopted by Indraratna et al. [24, 26] as well as Chrismer and Selig [25], the power law connection between the cumulative strain and its corresponding loading cycles can well predict the long-term deformation of granular soils. Most importantly, it can be easily implemented in the finite element analysis because of its explicit expression. To better take into account this power law phenomenon, the fractional derivative is employed here. For cyclic triaxial test as schematically illustrated by Fig. 1, the cumulative shear strain  $\varepsilon_s^p$  is assumed to result from the average deviator stress  $q^{av}$  [5] and have the following relationship:

$$\frac{d^\alpha \varepsilon_s^p}{dN^\alpha} = \frac{1}{rp_a} q^{av} \quad (8)$$

where the shear strain  $\varepsilon_s^p$  is fractionally differentiated by the number of loading cycles ( $N$ ) instead of the time  $t$ . This is because in the context of cyclic loading rate means a derivative with respect to the number,  $N$ . It should be noted that the number of load cycles,  $N$ , can be related to the real loading time,  $t$ , by using  $t = N / f$  where  $f$  denotes the load frequency. Similar approaches can be found elsewhere in [6, 8-10].  $r$  is the shear-related parameter, reflecting the long-term behavior of granular soils.  $p_a$  is the atmospheric pressure (101kPa), for the purpose of parameter dimensionless. Applying Laplace and inverse Laplace transformations to both sides of Eq. (8), yields

$$d\varepsilon_s^p = \frac{\alpha q^{av}}{\Gamma(1+\alpha)rp_a} N^{\alpha-1} \quad (9)$$

Eq. (9) is the ultimate correlation between the cumulative strain  $\varepsilon_s$  and the loading cycles,  $N$ . It offers mathematical representation for how the cumulative strain frequently manifests itself through the empirical formula with the form of a power-law function.

134

135

### III. CYCLIC FLOW RULE

136 Based on the principle of energy conservation, many different kinds of functions [32-34]  
 137 describing the static flow for various geomaterials have been deduced, for instance, the Rowe  
 138 dilatancy equation [32]. However, for granular soils which not only experience particle  
 139 arrangement but also particle breakage during loading [35]. The energy dissipated by particle  
 140 breakage for one individual loading process is assumed to be proportional to the energy  
 141 dissipated by particle arrangement as suggested by McDowell [36]. Therefore, the following  
 142 energy conservative equation is used:

$$143 \quad qd\varepsilon_s^p + p'd\varepsilon_v^p = Mp'd\varepsilon_s^p + Mp'd\varepsilon_s^p \frac{M^a - \eta^a}{\eta^a} \quad (10)$$

144 where  $p'$  ( $= \sigma'_1/3 + 2\sigma'_3/3$ ) is the mean effective principal stress. The stress ratio  $\eta = q/p'$ .  
 145  $M$  ( $= M_0 p'^b$ ) is the critical state friction parameter of the tested material.  $M_0$  and  $b$  are the  
 146 material constants. It was found that the shear and volumetric strains of soils tested under  
 147 cyclic loading flows according to a cyclic flow rule [6, 8]. Wichtmann et al. [8-10] proposed  
 148 a stress dilatancy equation by assuming that the energy was only dissipated by particle  
 149 slippage. However, as stated before, granular soils not only suffer particle arrangement but  
 150 also breakage during loading. Therefore, to better reflect the deformation mechanism, a  
 151 modified cyclic flow rule is suggested here by considering energy dissipation from both  
 152 particle rearrangement and breakage. For an arbitrary cyclic loading process, the total plastic  
 153 strain for the tested sample can be expressed as an integral of all the increments in Eq. (10).

$$154 \quad \int d\varepsilon_v^p = M^{a+1} \int \frac{1}{\eta^a} d\varepsilon_s^p - \int \eta d\varepsilon_s^p \quad (11)$$

155 The stress ratio,  $\eta$ , in Eq. (11) varies with time. However, it can be treated as a mean value,  
 156  $\eta_m$ , as suggested by Chang and Wichtmann [37].

$$157 \quad \eta_m = \frac{\int \eta d\varepsilon_s^p}{\int d\varepsilon_s^p} \quad (12)$$

$$158 \quad \eta_m^{-a} = \frac{\int \eta^{-a} d\varepsilon_s^p}{\int d\varepsilon_s^p} \quad (13)$$

159 Substituting Eqs. (12) and (13) into Eq. (11), one has

$$160 \quad \int d\varepsilon_v^p = \frac{M^{a+1} - \eta_m^{a+1}}{\eta_m^a} \int d\varepsilon_s^p \quad (14)$$

161 By rearranging Eq. (14), the relationship between the cumulative volumetric strain and the  
 162 the shear strain can be obtained as

$$163 \quad \frac{d\varepsilon_v^p}{d\varepsilon_s^p} \approx \frac{M^{a+1} - \eta_m^{a+1}}{\eta_m^a} \quad (15)$$

164 Eq. (15) can be regarded as a modified cyclic flow rule for granular soils considering the  
 165 influence of particle breakage. However, the value of the stress ratio,  $\eta_m$ , needs to be  
 166 determined before the actual use of Eq. (15) in capturing the flow direction of the cumulative  
 167 strains in granular soils. According to the laboratory observation by Chang and Wichtmann  
 168 [37],  $\eta_m$  is slightly larger than the averaged stress ratio,  $\eta^{av}$ , in cyclic loading. Therefore, the  
 169 averaged stress ratio,  $\eta^{av}$ , is used instead of the mean value,  $\eta_m$ .

$$170 \quad \frac{d\varepsilon_v^p}{d\varepsilon_s^p} = \frac{M^{a+1} - (\eta^{av})^{a+1}}{\beta(\eta^{av})^a} \quad (16)$$

171 where  $\beta$  is the material constant, diminishing the influence of the difference between the  
 172 mean stress ratio,  $\eta_m$ , and the averaged stress ratio,  $\eta^{av}$ , on the cyclic flow direction. Fig. 2  
 173 shows the comparison of the flow directions predicted by Eq. (16) and the modified Cam-  
 174 clay model suggested by Wichtmann et al. [9, 38]. The modified cyclic flow rule takes into  
 175 account the effect of particle breakage and thus gives better performance than that by  
 176 Wichtmann et al. [38], especially in the stress dilatant part where the trend of volumetric  
 177 dilation was reduced by the particle breakage occurred inside the sample.

178

#### 179 IV. CONSTITUTIVE EQUATIONS

180 The cumulative total strain is a sum of the elastic strain and the plastic strain, which can be  
 181 formulated as

$$182 \quad d\varepsilon_v = d\varepsilon_v^e + d\varepsilon_v^p \quad (17)$$

$$183 \quad d\varepsilon_s = d\varepsilon_s^e + d\varepsilon_s^p \quad (18)$$

184 where  $\varepsilon_v^e$  and  $\varepsilon_s^e$  are the resilient volumetric and shear strains, respectively. The resilient  
 185 parts of the total strains can be given as

$$186 \quad d\varepsilon_v^e = \frac{dp^{av}}{K} \quad (19)$$

$$187 \quad d\varepsilon_s^e = \frac{q^{av}}{3G} \quad (20)$$



188 where the shear modulus  $G$  can be defined as [39-40]

$$189 \quad G = G_0 \frac{(2.97 - e_0)^2}{1 + e_0} \sqrt{p^{\text{av}} p_a} \quad (21)$$

190 where  $e_0$  is the initial void ratio of the sample.  $P_a = 101$  kPa, is the atmospheric pressure.  $G_0$   
191 denotes the shear-related modulus for virgin loading;  $K$  is the bulk modulus that is expressed  
192 as

$$193 \quad K = K_0 \frac{(2.97 - e_0)^2}{1 + e_0} \sqrt{p^{\text{av}} p_a} \quad (22)$$

194 where  $K_0$  denotes the compression-related modulus for virgin loading;. The cumulative  
195 plastic strains caused by cyclic loading can be given as

$$196 \quad d\varepsilon_s^p = \frac{\alpha q^{\text{av}}}{\Gamma(1 + \alpha) r p_a} N^{\alpha-1} \quad (23)$$

$$197 \quad d\varepsilon_s^p = \frac{M^{a+1} - (\eta^{\text{av}})^{a+1}}{\beta (\eta^{\text{av}})^a} \frac{\alpha q^{\text{av}}}{\Gamma(1 + \alpha) r p_a} N^{\alpha-1} \quad (24)$$

198 where parameter  $r$  should depend not only on the soil type but also on the stress state and  
199 initial physical state. As suggested by Li et al. [41], it was not convenient to introduce the  
200 moisture content and dry density directly into the equation. However, the cyclic strain  
201 amplitude of the first loading cycle can indirectly represent the influence of the initial  
202 physical state on the cumulative strain of the granular soils. Thus, an empirical formula  
203 considering the influence of both stress state and initial physical state of soils is suggested as

$$204 \quad r = D (\eta^{\text{av}})^m (\varepsilon^{\text{ampl}})^n \quad (25)$$

205 where  $D$ ,  $m$ ,  $n$ , are material constants and the cyclic strain amplitude,  $\varepsilon^{\text{ampl}}$ , can be obtained  
206 by using

$$207 \quad \varepsilon^{\text{ampl}} = \frac{\Delta q}{G} \frac{1}{1 - \frac{2\Delta q}{\Delta q_{\text{max}}}} \quad (26)$$

208 where  $\Delta q$  and  $\Delta q_{\text{max}}$  denote the cyclic amplitude of the deviator stress and the distance away  
209 from the failure envelop, respectively, as illustrated in Fig. 1. Note that  $\Delta p'$  and  $p^{\text{av}}$  in Fig. 1  
210 are the cyclic amplitude of the mean principal stress and the averaged mean principal stress,  
211 respectively.

212

213

## V. MODEL PARAMETERS

214 This model contains ten parameters, i.e.,  $G_0$ ,  $\nu$ ,  $M_0$ ,  $a$ ,  $b$ ,  $\alpha$ ,  $\beta$ ,  $D$ ,  $m$  and  $n$ . All of them  
 215 can be determined by static and cyclic triaxial tests. The moduli  $K_0$  and  $G_0$  can be obtained by  
 216 resonant column test or measuring the initial stress-strain of the sample subjected to triaxial  
 217 loading. The critical state friction parameter  $M_0$  and  $b$  related to the gradient of the critical  
 218 state stress in the  $p$ - $q$  space and can be obtained by static triaxial test. The critical state stress  
 219 along with the peak stress envelop of railroad ballast, as shown in Fig. 3 varies with the initial  
 220 confining pressures which is different from that of sand [42-43]. This can be partially  
 221 attributed to the particle breakage during sample preparation which changed the initial  
 222 particle size distribution of the railroad ballast. The critical stress ratio,  $M$ , depends on the  
 223 effective mean principal stress [43-45]. An increase of stress level leads to an increase of the  
 224 particle breakage [46-48]. Therefore, a varying critical stress ratio as suggested by Xiao et al.  
 225 [43] is used. However, the critical state friction angle for sand [10] is taken as constant here.  
 226 Parameters  $a$  and  $\beta$  define the flow direction of sand under cyclic loading and can be  
 227 determined by adjusting the value of  $\beta$  to obtain a better correlation between  
 228  $\ln(d\varepsilon_v^p / d\varepsilon_s^p + \eta^{av} / \beta)$  and  $\ln(\eta^{av})$ , where the value of  $a$  can be obtained by measuring the  
 229 slope of the corresponding fitting line, as illustrated in Fig. 4. The fractional derivative order,  
 230  $\alpha$ , describes the rate of strain accumulation and is independent of the deviator stress  
 231 according to the research by Li et al. [41]. Therefore, it can be determined by fitting the  
 232 relationship between the shear strain,  $\varepsilon_s^p$ , and the number of loading cycles,  $N$ . Note that  
 233 sometimes the cumulative strain used to calculate the exponent,  $\alpha$ , as illustrated in Fig. 5, is  
 234 the cumulative total strain rather than the cumulative plastic strain. This is considered  
 235 acceptable because the resilient/elastic strain will become nearly constant and negligible  
 236 when compared with the plastic strain after a certain number of loading cycles. Parameters  $D$ ,  
 237  $m$ , and  $n$  can be obtained by regression with the value of  $r$  (Fig. 6) which is related to the  
 238 plastic strain of the first loading cycle. To show the advantage of the present model in  
 239 simulating the cumulative deformation, the prediction of the mathematical model proposed  
 240 by François et al. [46] is also provided for comparison. The model contains 10 parameters  
 241 (Table 1) that depend on the value of the cyclic stress amplitude. As suggested by François et  
 242 al. [49], the model parameters need to be determined by nonlinear least squares method.  
 243 Detailed values of the model parameters can be found in Table 1.

244

245

## VI. MODEL PERFORMANCE

246 It was found that the stress amplitude had significant influence on the cyclic deformation  
 247 of granular soils in the long run [8-10]. To validate the proposed mathematical model, test  
 248 results of four different granular soils, as shown in Table 2, are used. The natural quartz sand  
 249 was taken from a sand pit near Dorsten, Germany [10]. The grain shape is sub-angular and  
 250 the specific weight along with the other physical properties can be found in Table 2. The  
 251 samples were tested under different drained cyclic triaxial loading conditions with the  
 252 averaged mean principal stress equal 200 kPa and the averaged deviator stresses equal to 50  
 253 kPa, 100 kPa, 150 kPa, 175 kPa, and 225 kPa. Each loading condition had the same cyclic  
 254 stress amplitude  $q^{\text{ampl}}$ , equal to 40 kPa, and the same loading frequency, equal to 1 Hz. Fig. 7

255 shows the model simulation of the cumulative deformations of natural quartz sand [10]. The  
256 cumulative strain increased with the increase of the applied average stress ratio. It is observed  
257 that the mathematical model can well capture both the long-term shear strain and volumetric  
258 strain under different deviator stresses. It can also give satisfactory predictions of the initial  
259 deformations for several test conditions. However, if more different complicated loading  
260 conditions involved, this model indeed loses some ability in accurately predicting the  
261 deformation at the initial loading stage, for example, test result with higher stress ratio. This  
262 is because this model aims at predicting the long-term cumulative deformation rather than the  
263 short-term stress strain response of the sample. However, this shortcoming can be resolved by  
264 using variable fractional derivative order but is not within the scope of current research. To  
265 the author's knowledge, the fractional derivative order could depend on the mechanical state,  
266 such as the loading stress and strain, etc. [27-29]. But, the use of the variable order may  
267 involve significantly complex mathematic calculations (see [27] for instance), which is not  
268 applicable for the engineering concern. The predictions of the numerical model, denoted as  
269 François model [46], are also provided for comparison. As shown in Fig. 7, it can only give  
270 comparatively good predictions of the soil deformation under low stress ratios. In contrast,  
271 the proposed model exhibits better potential in characterising the cumulative deformation of  
272 the natural quartz sand under both low and high stress ratios.

273 The railroad ballast was a kind of crushed basalt, collected from Bombo quarry near  
274 Wollongong, New South Wales, Australia. It was an angular/subangular volcanic latite basalt  
275 that contains the primary minerals feldspar, plagioclase, and augite [42]. Its physical  
276 attributes can be found in Table 2. The railroad ballast was tested under the confining  
277 pressures equal to 10 kPa, 60 kPa, 120 kPa with two different cyclic stress amplitudes equal  
278 to 185 kPa and 455 kPa. The sample was prepared by tamping to 300 mm in diameter and  
279 600 mm in height before tested under a loading frequency equal to 20 Hz. Fig. 8 shows the  
280 comparison between the test results and the predicted results by the proposed model as well  
281 as the François model. It is observed from Fig. 8(a) that the proposed model can well capture  
282 the cumulative shear strain of ballast tested under different confining and deviator stresses.  
283 The cumulative shear strain increased with increasing confining pressure. Larger deviator  
284 stress resulted in larger cumulative shear strain given the same confining pressure. Moreover,  
285 through the incorporation of the modified cyclic flow rule, the proposed model can well  
286 characterize both the volumetric dilatancy under low confining pressure and the volumetric  
287 contraction under relatively high confining pressure, as shown in Fig. 8(b). But in contrast,  
288 the François model can only give satisfactory predictions of the shear strains under low  
289 confining pressure and the volumetric strains under high confining pressure. Most  
290 importantly, the model parameters are highly dependent on the cyclic amplitude. Therefore,  
291 the proposed model exhibits a better flexibility in modelling the long-term deformation of  
292 different granular soils tested under different loading conditions.

293 Moreover, to preliminarily demonstrate the ability of the fractional order model in  
294 characterising the entire stress strain hysteresis curve, two additional cyclic tests, as shown in  
295 Figs. 9 and 10, are simulated by using Eq (7). Fig. 9 shows the prediction of the drained  
296 cyclic triaxial tests on the Zipingpu rockfill [14]. The sample was prepared to have a diameter

297 equal to 300 mm and a height equal to 600 mm before initially compressed to an effective  
298 mean principal stress equal to 500 kPa. The subsequent test was conducted under the stress  
299 amplitude equal to 400 kPa. The physical properties of the sample can be found in Table 2.  
300 The shear-related moduli,  $G_0$ , used for first, second loading and the subsequent unloading are  
301 15.5 MPa, 9.7 MPa, 7.0 MPa, respectively. The compression-related moduli,  $K_0$ , used for first,  
302 second loading and the subsequent unloading are 42.3 MPa, 5.5 MPa, and 1.0 MPa,  
303 respectively. The fractional order  $\alpha$  is found to be 0.71. It is observed from Fig. 9(a) that the  
304 proposed approach can well represent the virgin loading and unloading of the Zipingpu  
305 rockfill. The subsequent hysteresis loops between the axial strain and the deviator stress can  
306 be also characterised. However, as shown in Fig. 9(b), the proposed model can only simulate  
307 the increase of the volumetric strain during virgin loading. The subsequent variation cannot  
308 be well simulated. Fig. 10 shows the prediction of the triaxial test results performed on a dense  
309 rockfill [22] which consisted of mainly weathered quartz monzonite. The triaxial test was  
310 performed on a 300 mm diameter and 700 mm high specimen. The initial effective mean  
311 principal stress was equal to 3 MPa and the subsequent loading amplitude was 2MPa with a  
312 loading frequency equal 0.1 Hz. Detailed physical properties of the Toyoura sand can be  
313 found in Table 2. The shear-related moduli,  $G_0$ , used for first, second loading and the  
314 subsequent unloading are 32 MPa, 7.1 MPa, 9.5 MPa, respectively. The compression-related  
315 moduli,  $K_0$ , used for first, second, loading and the subsequent unloading are 5.82 MPa, 4.0  
316 MPa, and 0.58 MPa, respectively. The fractional order  $\alpha = 0.81$ . Once again, a well  
317 representation of the stress strain hysteresis can be observed from Fig. 10(a). But the  
318 predicted volumetric strain is relatively higher than the experimental results. Further  
319 modification of the current model needs to be conducted in order to accurately capture the  
320 variation of the volumetric strain during cyclic loading.

321

322

## VII. CONCLUSIONS

323 A fractional order model was presented to simulate the cumulative deformation of  
324 granular soils subjected to cyclic loading. This model consists of two main parts. Firstly, a  
325 fractional derivative was used to derive the power law connection between the cumulative  
326 shear strain and its loading cycles. Then, an energy based approach was employed to provide  
327 a modified cyclic flow rule particularly for crushable granular soils. The modified the flow  
328 rule took into account the particle breakage of granular soils under cyclic loading thus had a  
329 better potential in characterizing the cyclic flow direction of granular soils. All the model  
330 parameters can be determined from the cyclic and static triaxial tests. It is noted that the  
331 physical origins of several parameters are not clear and still need further investigation. To  
332 validate the proposed model, predicted and measured results for several different granular  
333 soils, i.e., sand, rockfill, and railroad ballast, were simulated. The proposed model was also  
334 compared with an existing cumulative model to demonstrate its advantage in modelling long-  
335 term deformation of granular soils. It was observed that with the help of the fractional  
336 derivative theory, the distinct power law evolution between the shear strain and the  
337 corresponding loading cycle under different loading conditions was reasonably captured.  
338 Besides, by employing the modified cyclic flow rule, the model was also able to predict both

339 the volumetric compression under relatively high confining pressure and the volumetric  
340 dilatancy under low confining pressure. It is thus concluded that the proposed model could  
341 well capture both the cumulative shear strain and the cumulative volumetric strain of granular  
342 soils. Moreover, to preliminary demonstrate the fractional order approach in modelling the  
343 stress strain hysteresis during cyclic loading, two additional simulations of the triaxial test  
344 results performed on rockfill were also provided. The fractional order approach was shown to  
345 have great potential in modelling the entire stress and strain curve of rockfill during cyclic  
346 loading. However, this model cannot accurately represent the variation of the volumetric  
347 deformation. Further modifications still need be conducted.

348

349

#### ACKNOWLEDGEMENTS

350 The authors would like to thank Professor W. Chen and Dr Xiaodi Zhang in Hohai  
351 University for their kind instructions on several fundamentals of the fractional calculus. The  
352 financial supports provided by the Fundamental Research Funds for the Central Universities  
353 (Grant No. 106112015CDJXY200008) is also greatly appreciated.

354

355

#### REFERENCES

- 356 [1] Miura,N., Fujikawa,K., Sakai,A. and Hara,K. Field measurement of settlement in saga  
357 airport highway subjected to trafficload. *Tsuchi-to-Kiso*, 1995, 43-6(449): 49–51.
- 358 [2] Ren,X.W., Tang,Y.Q., Li,J. and Yang,Q. A prediction method using grey model for  
359 cumulative plastic deformation under cyclic loads. *Natural Hazards*, 2012, 64(1): 441–457.
- 360 [3] Li,D.Q. and Selig,E.T. Cumulative plastic deformation for fine grained subgrade soils.  
361 *Journal of Geotechnical Engineering ASCE*, 1996, 122(12): 1006–1013.
- 362 [4] Chai,J.C. and Miura,N. Traffic-load-induced permanent deformation of road on soft  
363 subsoil. *Journal of Geotechnical and Geoenvironmental Engineering*, 2002, 128(11): 907–  
364 916.
- 365 [5] Bouckovalas,G., Whitman,R.V. and Marr,W.A. Permanent displacement of sand with  
366 cyclic loading. *Journal of Geotechnical Engineering ASCE*, 1984, 110(11): 1606–1623.
- 367 [6] Suiker,A.S.J. and de,Borst,R. A numerical model for the cyclic deterioration of railway  
368 tracks. *International Journal for Numerical Methods in Engineering*, 2003, 57(4), 441–  
369 470.
- 370 [7] Khalili,N., Habte,M. and Valliappan,S. A bounding surface plasticity model for cyclic  
371 loading of granular soils. *International Journal for Numerical Methods in Engineering*,  
372 2005, 63(14), 1939–1960.
- 373 [8] Niemunis,A., Wichtmann,T. and Triantafyllidis,T.H. A high-cycle accumulation model for  
374 sand. *Computer and Geotechnics*, 2005, 32(4): 245–263.
- 375 [9] Wichtmann,T., Niemunis,A. and Triantafyllidis,T.H. Experimental evidence of a unique  
376 flow rule of non-cohesive soils under high-cyclic loading. *Acta Geotechnica*, 2006, 1(1):  
377 59–73.

- 378 [10] Wichtmann,T., Niemunis,A. and Triantafyllidis,T.H. Validation and calibration of a high-  
379 cycle accumulation model based on cyclic triaxial tests on eight sands. *Soils and*  
380 *Foundations*, 2009, 49(5), 711–728.
- 381 [11] Li,S., and Huang,M. Undrained long-term cyclic degradation characteristics of offshore  
382 soft clay. *In Proceedings of the GeoShanghai 2010 International Conference, Shanghai,*  
383 *China. Huang M S, Yu X, Huang Y, eds. 2010. 263–271.*
- 384 [12] Li,L.L., Dan,H.B. and Wang,L. Z. Undrained behavior of natural marine clay under cyclic  
385 loading, *Ocean Engineering*, 2011, 38(16): 1792–1805.
- 386 [13] Karim,M.R., Oka,F., Krabbenhoft,K., Leroueil,S. and Kimoto,S. Simulation of long-term  
387 consolidation behavior of soft sensitive clay using an elasto-viscoplastic constitutive  
388 model. *International Journal for Numerical and Analytical Methods in Geomechanics*,  
389 2013, 37(16): 2801–2824.
- 390 [14] Liu,H., Zou,D. and Liu,J. Constitutive modeling of dense gravelly soils subjected to cyclic  
391 loading. *International Journal for Numerical and Analytical Methods in Geomechanics*,  
392 2014, DOI: 10.1002/nag.2269.
- 393 [15] Seidalinov,G. and Taiebat,M. Bounding surface SANICLAY plasticity model for cyclic  
394 clay behavior. *International Journal for Numerical and Analytical Methods in*  
395 *Geomechanics*, 2014, 38(7): 702–724.
- 396 [16] Ishikawa,T., Sekine,E. and Miura,S. Cyclic deformation of granular material subjected to  
397 moving-wheel loads. *Canadian Geotechnical Journal*, 2011, 48(5): 691–703.
- 398 [17] Suiker,A.S.J, Selig,E.T. and Frenkel,R. Static and cyclic triaxial testing of ballast and  
399 subballast. *Journal of Geotechnical and Geoenvironmental Engineering*, 2005, 131(6):  
400 771–782.
- 401 [18] Indraratna,B., Lackenby,J. and Christie,D. Effect of confining pressure on the degradation  
402 of ballast under cyclic loading. *Géotechnique*, 2005, 55(4): 325–328.
- 403 [19] Lackenby,J., Indraratna,B., McDowell,G. and Christie,D. Effect of confining pressure on  
404 ballast degradation and deformation under cyclic triaxial loading. *Géotechnique*, 2007,  
405 57(6): 527–536.
- 406 [20] Indraratna,B., Thakur,P.K. and Vinod,J.S. Experimental and numerical study of railway  
407 ballast behavior under cyclic loading. *International Journal of Geomechanics*, 2009, 10(4):  
408 136–144.
- 409 [21] Xiao,Y., Liu,H., Chen,Y. and Jiang,J. Bounding surface model for rockfill materials  
410 dependent on density and pressure under triaxial stress conditions. *Journal of Engineering*  
411 *Mechanics*, 2014, 140(4), 04014002. doi: 10.1061/(ASCE)EM.1943-7889.0000702.
- 412 [22] Fu,Z., Chen,S. and Peng,C. Modeling cyclic behavior of rockfill materials in a framework  
413 of generalized plasticity.*International Journal of Geomechanics*, 2014, 14(2): 191–204.
- 414 [23] Ling,H.I. and Yang,S. Unified sand model based on the critical state and generalized  
415 plasticity. *Journal of Engineering Mechanics*, 2006, 132(12): 1380–1391.
- 416 [24] Indraratna,B., Thakur,P.K., Vinod,J.S. and Salim,W. Semi-empirical cyclic densification  
417 model for ballast incorporating particle breakage. *International Journal of Geomechanics*,  
418 2012, 12(3): 260–271.
- 419 [25] Chrimer,S. and Selig,E.T. Computer model for ballast maintenance planning. *In*  
420 *Proceedings of 5th International Heavy Haul Railway Conference, Beijing, China. 1993,*  
421 *223–227.*

- 422 [26] Indraratna,B., Salim,W., Ionescuc,D. and Christie,D. Stress-strain and degradation  
423 behavior of railway ballast under static and dynamic loading, based on large-scale triaxial  
424 testing. *In Proceedings of 15th international conference on soil mechanics and*  
425 *geotechnical engineering, Istanbul, Turkey, 2001, 2093–2096.*
- 426 [27] Sun,H.G., Chen,W. and Chen,Y.Q. Variable-order fractional differential operators in  
427 anomalous diffusion modeling, *Physica A*, 2009, 388(21): 4586–4592.
- 428 [28] Sun,Y., Liu,H., Xiao,Y. Gao,H. and Cui,Y. Modeling of rheological behavior of  
429 geomaterials based on fractional viscoelastic equation with variable parameters. *In*  
430 *Proceedings of GeoHunan international conference 2011, Hunan, China. Ge L, Zhang X,*  
431 *Wu J, Correia A G, eds. 2011. 107–114.*
- 432 [29] Yin,D., Wu,H., Cheng,C. and Chen,Y.Q. Fractional order constitutive model of  
433 geomaterials under the condition of triaxial test. *International Journal for Numerical and*  
434 *Analytical Methods in Geomechanics*, 2013, 37(8): 961–972.
- 435 [30] Yin,D., Duan,X. and Zhou,X. Fractional time-dependent deformation component models  
436 for characterizing viscoelastic Poisson's ratio. *European Journal of Mechanics A/Solids*,  
437 2013, 42: 422–429.
- 438 [31] Kilbas,A.A.A, Srivastava,H.M. and Trujillo,J.J. Theory and applications of fractional  
439 differential equations. Elsevier Science Limited, 2006. 91–99.
- 440 [32] Rowe,P.W. The stress-dilatancy relation for static equilibrium of an assembly of particles  
441 in contact. *Proceedings of Royal Society of London A Mathematical and Physical Science*,  
442 1962, 269(1339): 500–527.
- 443 [33] Indraratna,B. and Salim,W. Modelling of particle breakage of coarse aggregates  
444 incorporating strength and dilatancy. *Proceedings of ICE Geotechnical Engineering*, 2002,  
445 155(4): 243–252.
- 446 [34] Sun,Y., Liu,H. and Yang,G. Yielding function for coarse aggregates considering gradation  
447 evolution induced by particle breakage. *Rock and Soil Mechanics*, 2013, 34(12): 3479–  
448 3484.
- 449 [35] Liu,H., Sun,Y., Yang,G. and Chen,Y. A review of particle breakage characteristics of  
450 coarse aggregates. *Journal of Hohai University (Natural Sciences)*. 2012, 40(4): 361–369.  
451 (in Chinese).
- 452 [36] McDowell,G.R. A family of yield loci based on micro mechanics. *Soils and Foundations*,  
453 2000, 40(6): 133–137.
- 454 [37] Chang,C.S and Whitman,R.V. Drained permanent deformation of sand due to cyclic  
455 loading. *Journal of Geotechnical Engineering ASCE*, 1988, 114(10): 1164–1180.
- 456 [38] Wichtmann,T., Niemunis,A.and Triantafyllidis,T.H. Flow rule in a high-cycle  
457 accumulation model backed by cyclic test data of 22 sands. *Acta Geotechnica*, 2014, 1–15.
- 458 [39] Richart,F.E.Jr, Hall,J.R. and Woods,R.D. Vibrations of soils and foundations. Englewood  
459 Cliffs, NJ: Prentice-Hall, 1970.
- 460 [40] Li,X. and Dafalias,Y. Dilatancy for cohesionless soils. *Géotechnique*, 2000, 50(4), 449–  
461 460.
- 462 [41] Li,D. and Selig,E.T. Cumulative plastic deformation for fine-grained subgrade soils.  
463 *Journal of Geotechnical Engineering ASCE*, 1996, 122(12): 1006–1013.

- 464 [42] Lackenby, J. Triaxial behaviour of ballast and the role of confining pressure under cyclic  
465 loading. Dissertation for the Doctoral Degree. Wollongong: University of Wollongong,  
466 2006. 89–91.
- 467 [43] Xiao, Y., Liu, H., Chen, Y., Jiang, J., and Zhang, W. State-dependent constitutive model for  
468 rockfill materials. *International Journal of Geomechanics*, 2014, 04014075. doi:  
469 10.1061/(ASCE)GM.1943-5622.0000421.
- 470 [44] Indraratna, B., Wijewardena, L.S.S. and Balasubramaniam, A.S. Large-scale triaxial testing  
471 of greywacke rockfill. *Géotechnique*, 1993, 43(1), 37–51.
- 472 [45] Frossard, E., Dano, C., Hu, W., and Hicher, P.Y. Rockfill shear strength evaluation: a  
473 rational method based on size effects. *Géotechnique*, 2012, 62(5), 415–427.
- 474 [46] Xiao, Y., Liu, H., Chen, Y., and Jiang, J. Bounding Surface Plasticity Model Incorporating  
475 the State Pressure Index for Rockfill Materials. *Journal of Engineering Mechanics*, 2014,  
476 140(11), 04014087. doi: 10.1061/(ASCE)EM.1943-7889.0000802.
- 477 [47] Xiao, Y., Liu, H., Chen, Y., Jiang, J. and Zhang, W. Testing and modeling of the state-  
478 dependent behaviors of rockfill material. *Computers and Geotechnics*, 61(9), 153–165.
- 479 [48] Xiao, Y., Sun, Y., and Hanif, F. A particle-breakage critical state model for rockfill material.  
480 *Science China Technological Sciences*, 58(7), 1125-1136.
- 481 [49] François, S., Karg, C., Haegeman, W., and Degrande, G. A numerical model for foundation  
482 settlements due to deformation accumulation in granular soils under repeated small  
483 amplitude dynamic loading. *International Journal for Numerical and Analytical Methods*  
484 *in Geomechanics*, 2010, 34(3): 273-296.
- 485



**Table caption list:**

Table 1 Model parameters

Table 2 Physical properties of the granular soils

Table 1. Model parameters

Model	Parameters	Natural quartz sand [10]	Railroad ballast [42]		
Current model	$q^{\text{ampl}}$ (kPa)	40	185	455	
	$G_0$ (kPa)	230	383	383	
	$K_0$ (kPa)	213	355	355	
	$M$	1.28	4.66	4.66	
	$b$	0	0.82	0.82	
	$a$	1.64	1.8	1.8	
	$\alpha$	0.15	0.1	0.1	
	$\beta$	0.55	1.0	1.0	
	$D$	1477.34	318.8	318.8	
	$m$	0.56	-1.1	-1.1	
	$n$	-0.21	-0.72	-0.72	
	François model [49]	$\alpha_f$ ( $10^{-4}$ )	0.007	7.4	2.6
		$\beta_f$ ( $10^{-6}$ )	-0.07	-5.4	-21.8
$\eta_f$		700	105.9	7.0	
$d_f$		0.25	0.01	0.01	
$\alpha_c$ ( $10^{-4}$ )		0.04	8.0	0.56	
$\beta_c$ ( $10^{-6}$ )		-0.02	-78	-3.4	
$\eta_c$		700	1.1	85.7	
$C_p$ ( $\text{Pa}^{-1}$ )		0.005	0.007	0.007	
$K_{ref}$		213	355	355	
$\nu$		0.2	0.2	0.2	

Table 2. Physical properties of the granular soils

Materials	Natural quartz sand [10]	Zipingpu rockfill [14]	Weathered monzonite [22]	Railroad ballast [42]
$G_s$	2.65	-	2.71	2.66
$d_{50}$ (mm)	0.35	9.5	18	39.5
$C_u$	1.9	-	11	1.53
$e_{max}$	0.930	-	0.3	0.97
$e_{min}$	0.544	-	0.15	0.67
$e_0$	0.745	0.313	0.17	0.74

### **Figure caption list:**

Fig. 1. Schematic representation of the cyclic triaxial test

Fig. 2. Cyclic flow rule

Fig. 3. Critical state line and peak stress line

Fig. 4. Determination of parameters  $a$  and  $\beta$

Fig. 5. Determination of exponent  $\alpha$

Fig. 6. Determination of parameters  $D$ ,  $m$  and  $n$

Fig. 7. Model predictions of the cumulative deformation of natural quartz sand [10]

Fig. 8. Model predictions of the cumulative deformation of railroad ballast [42]

Fig. 9. Representation of the stress strain behaviour of Zipingpu rockfill [14]

Fig. 10. Representation of the stress strain behaviour of weathered monzonite [22]

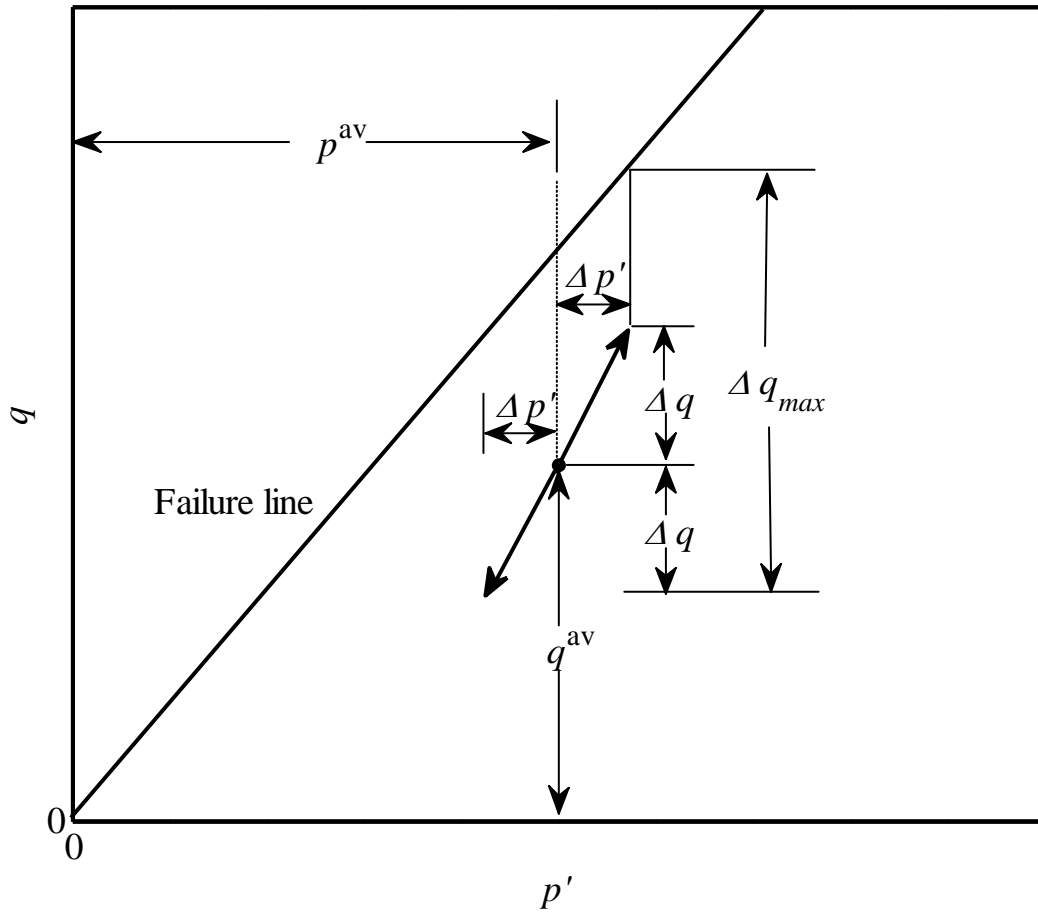


Fig. 1. Schematic representation of the cyclic triaxial test

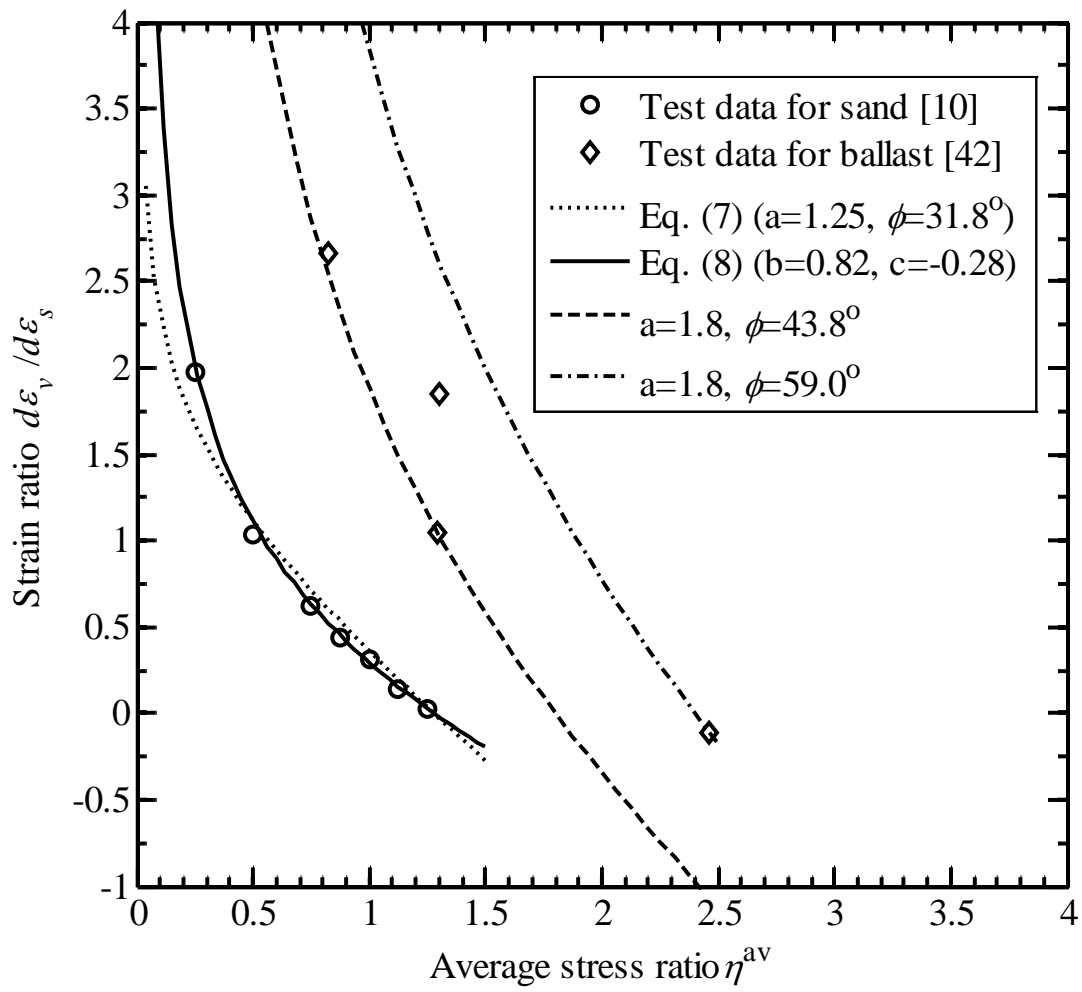


Fig. 2. Cyclic flow rule

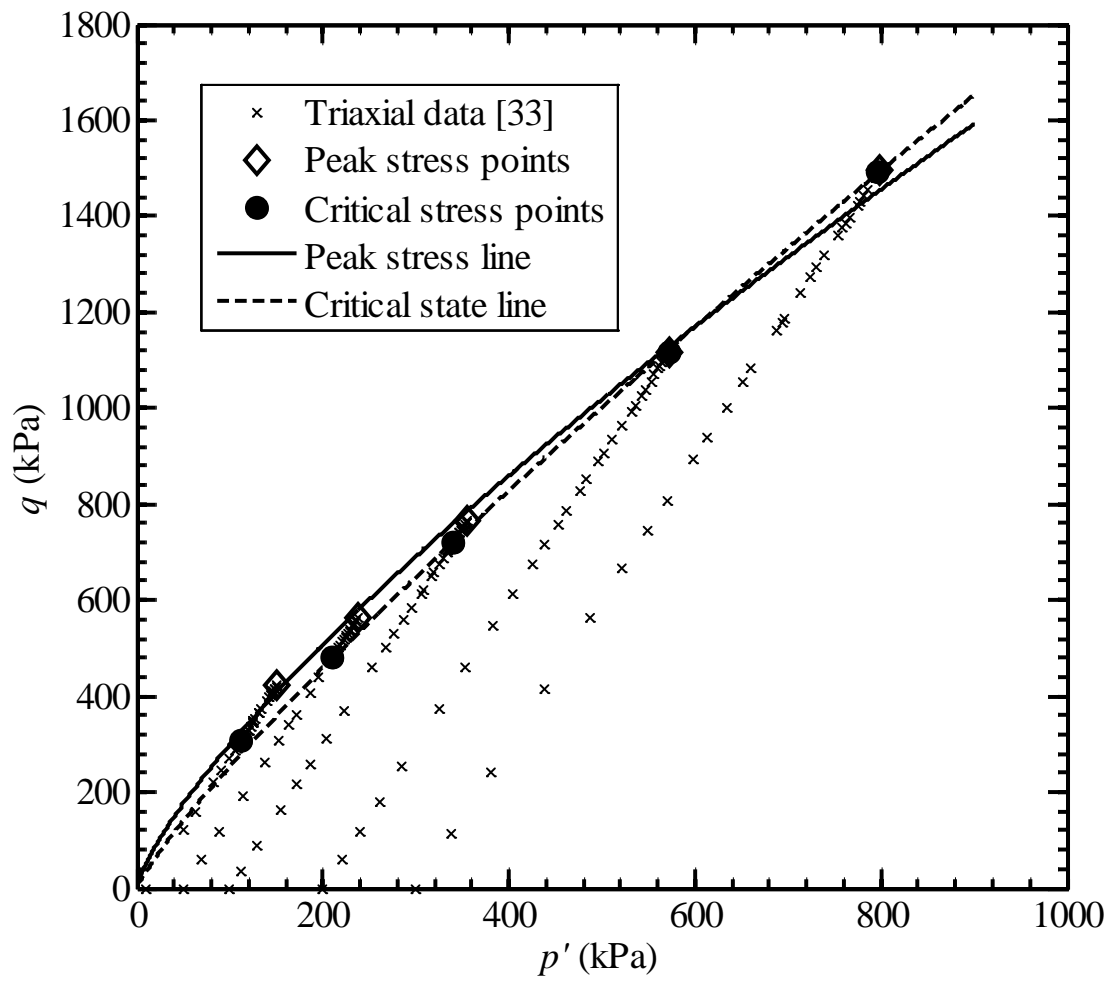


Fig. 3. Critical state line and peak stress line

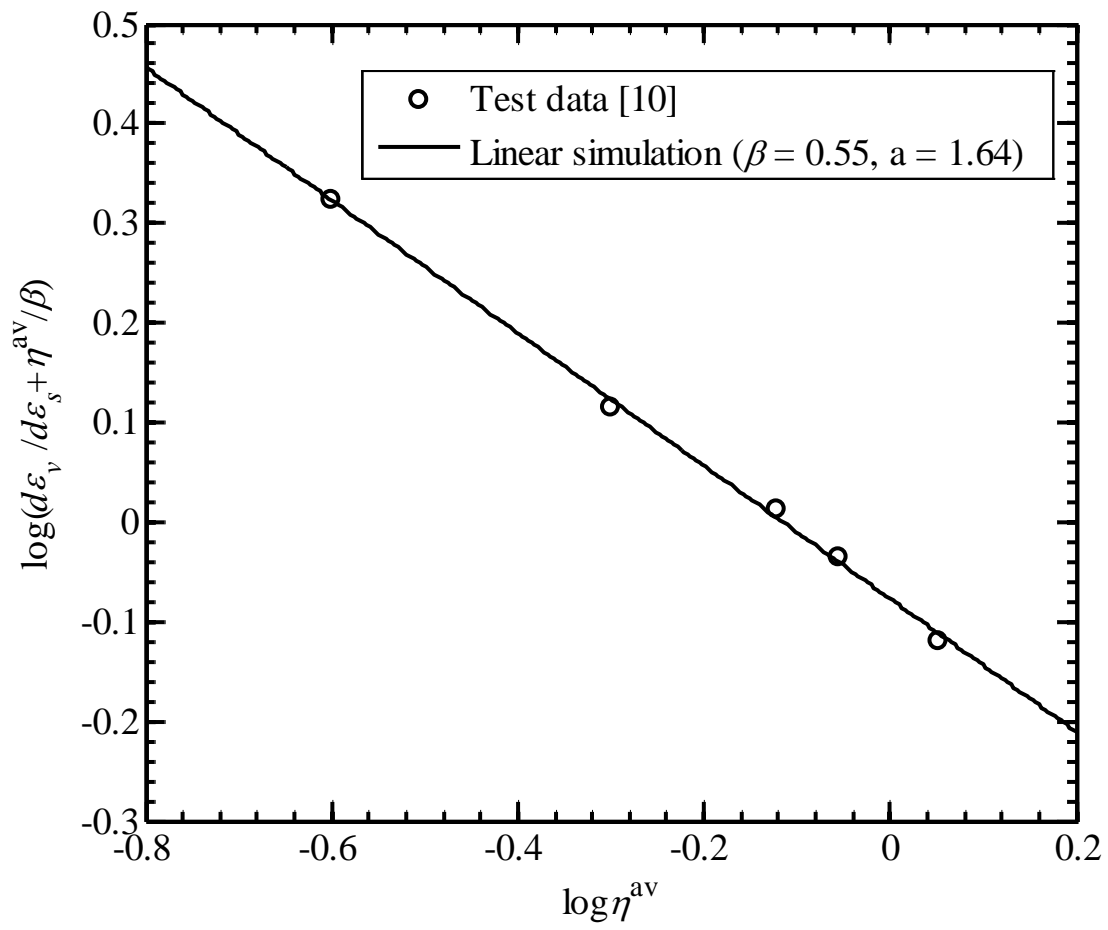


Fig. 4. Determination of parameters  $a$  and  $\beta$

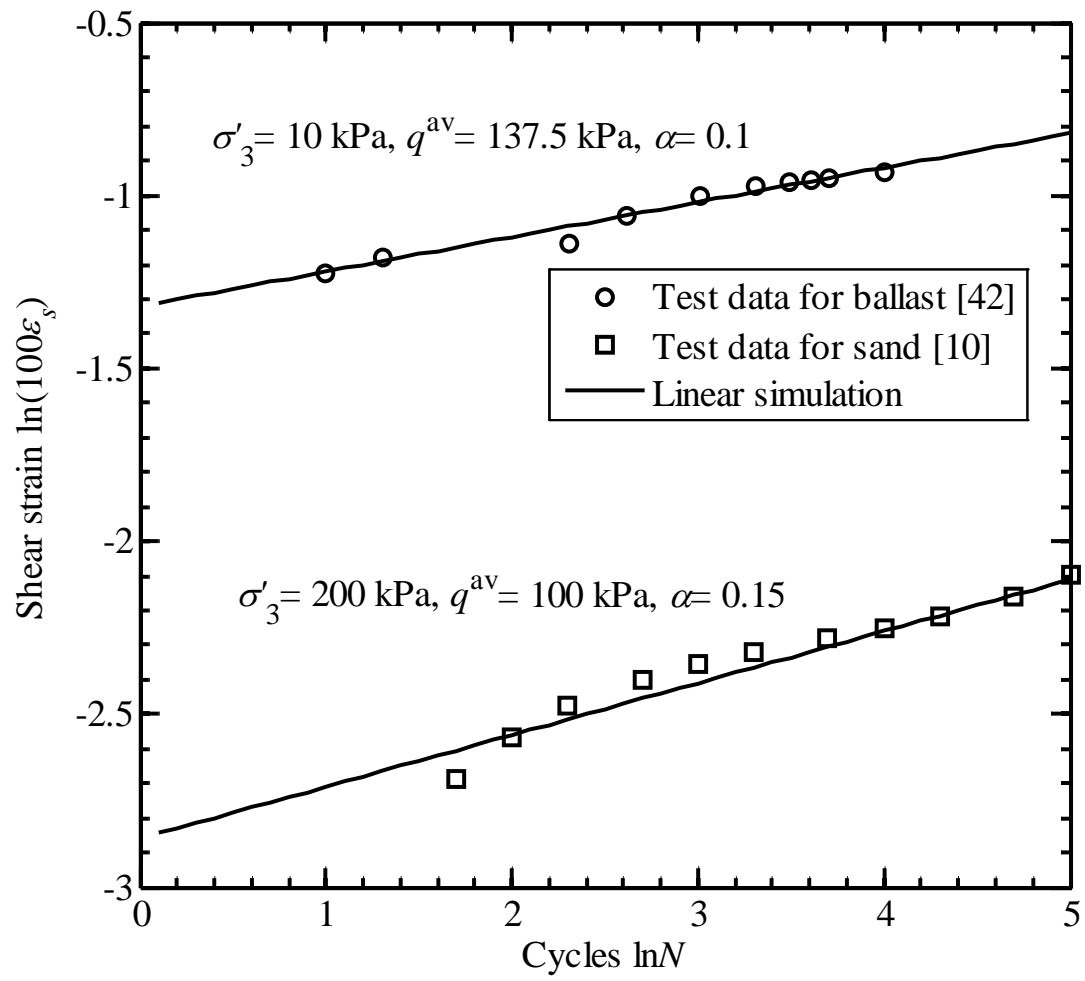


Fig. 5. Determination of exponent  $\alpha$



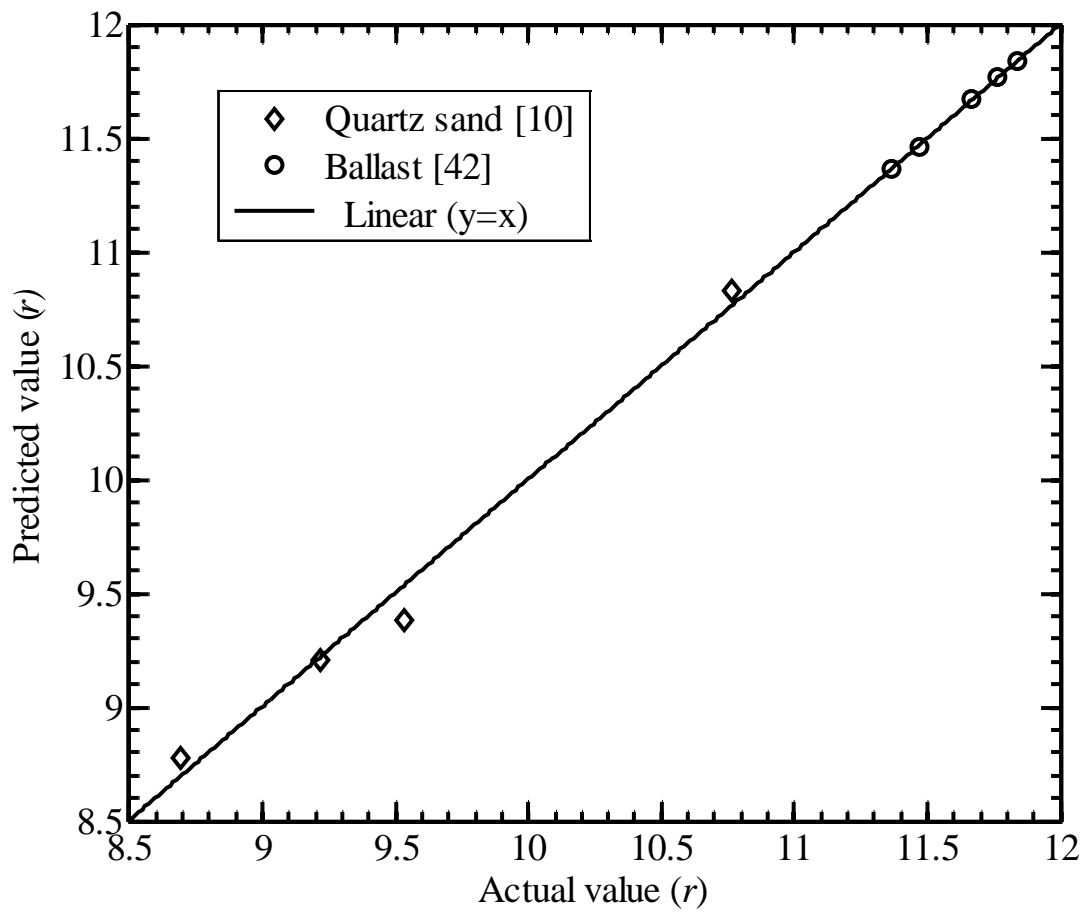


Fig. 6. Determination of parameters  $D$ ,  $m$  and  $n$

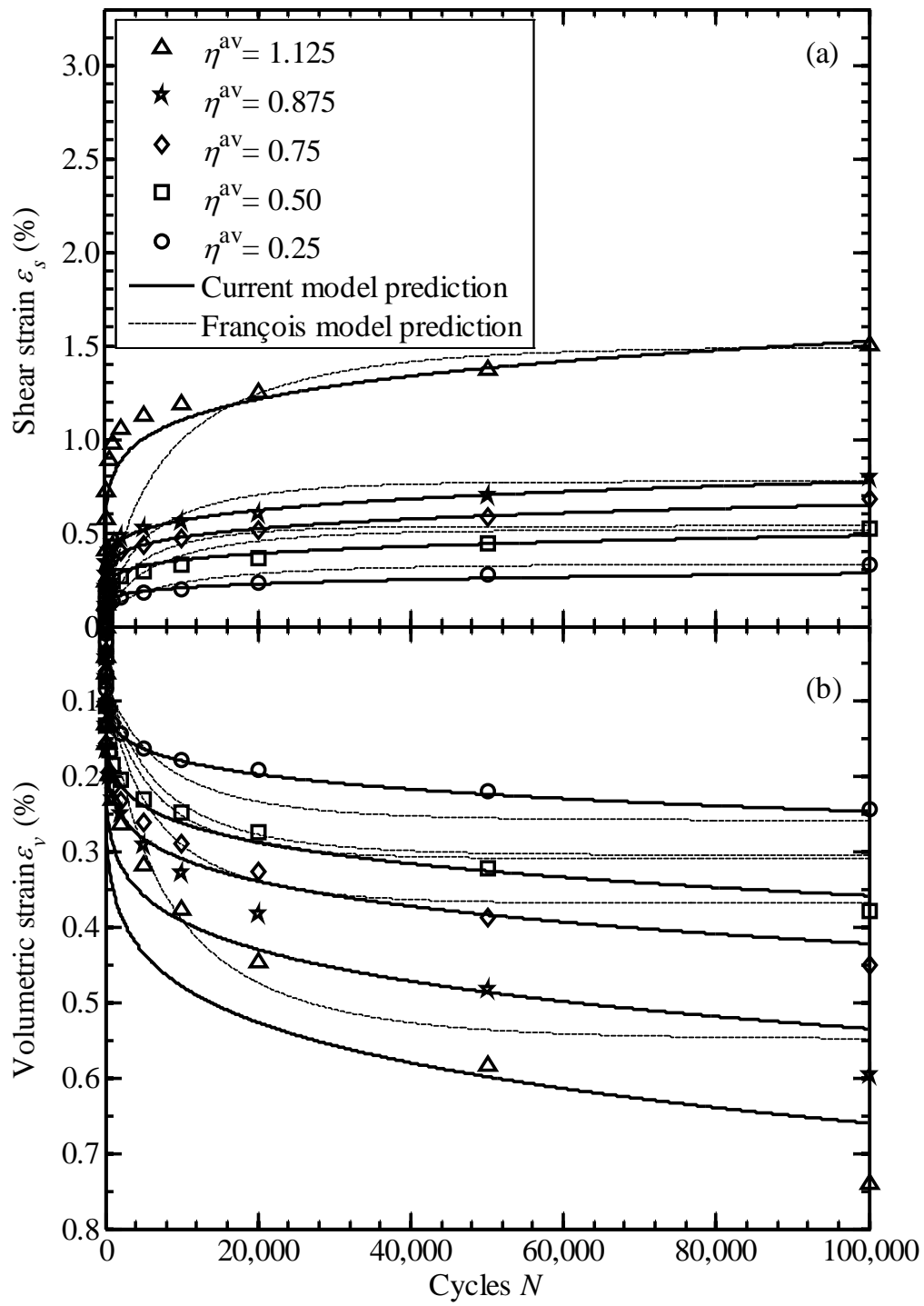


Fig. 7. Model predictions of the cumulative deformation of natural quartz sand [10]

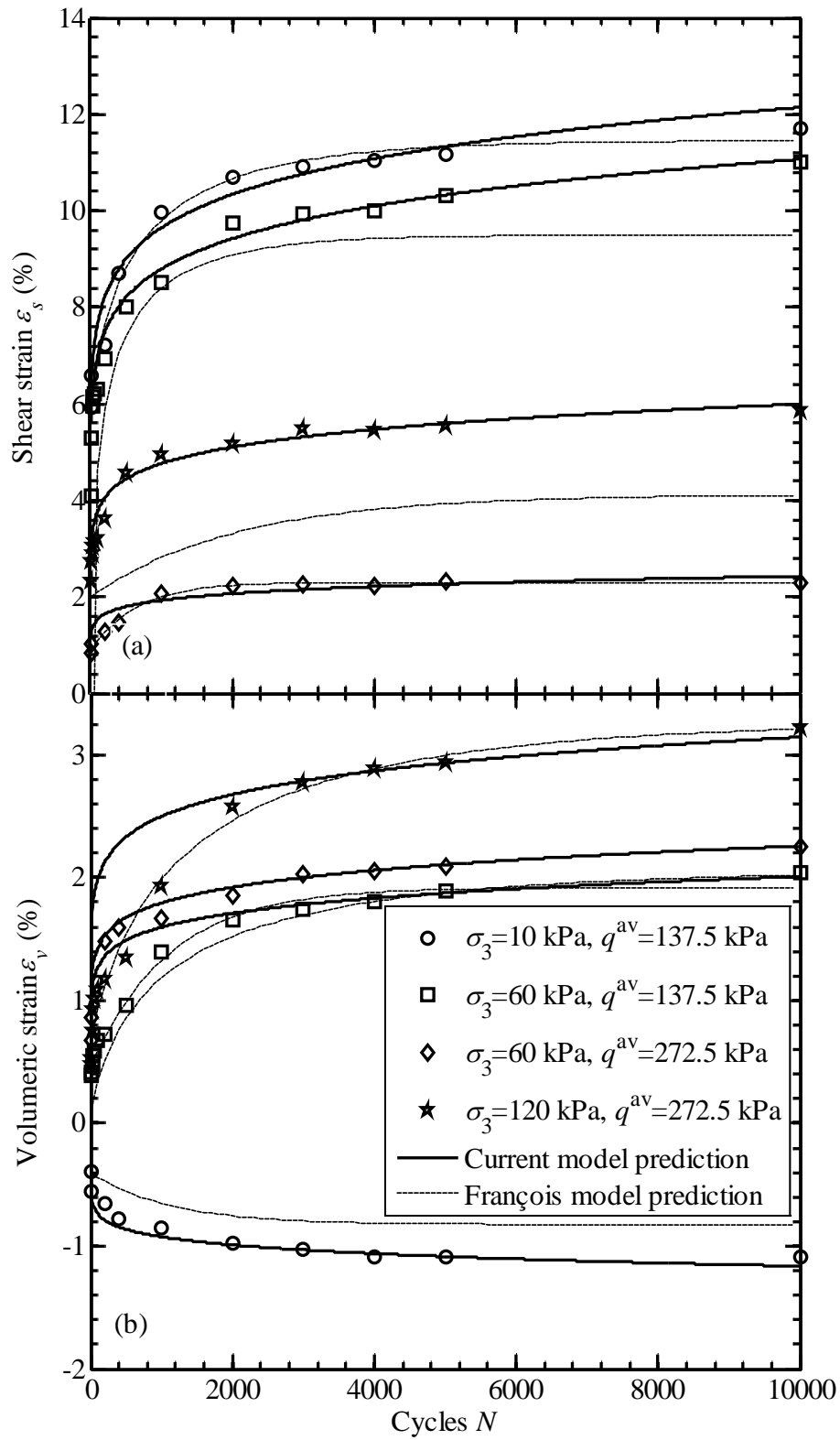


Fig. 8. Model predictions of the cumulative deformation of railroad ballast [42]

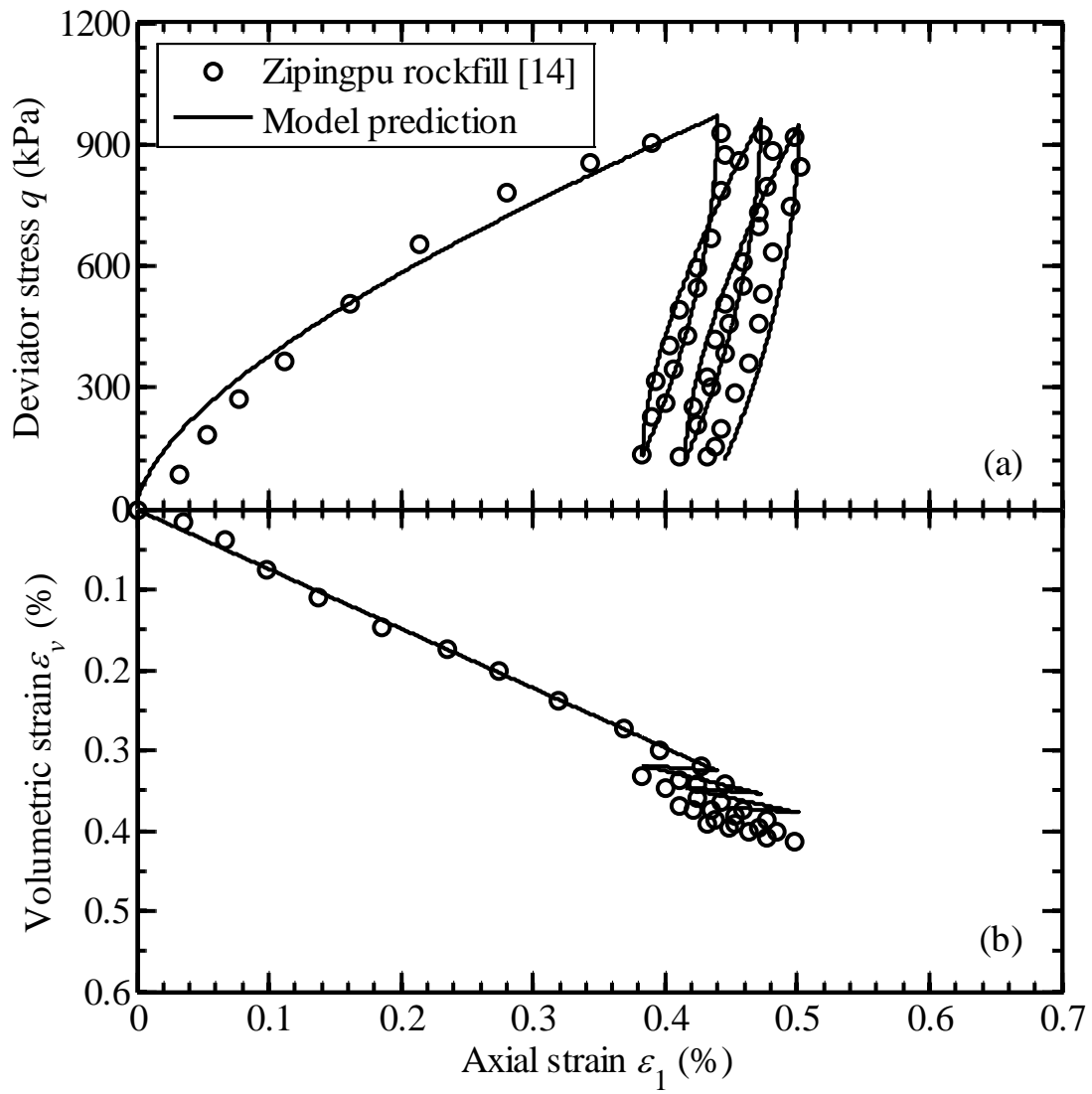


Fig. 9. Representation of the stress strain behaviour of Zipingpu rockfill [14]

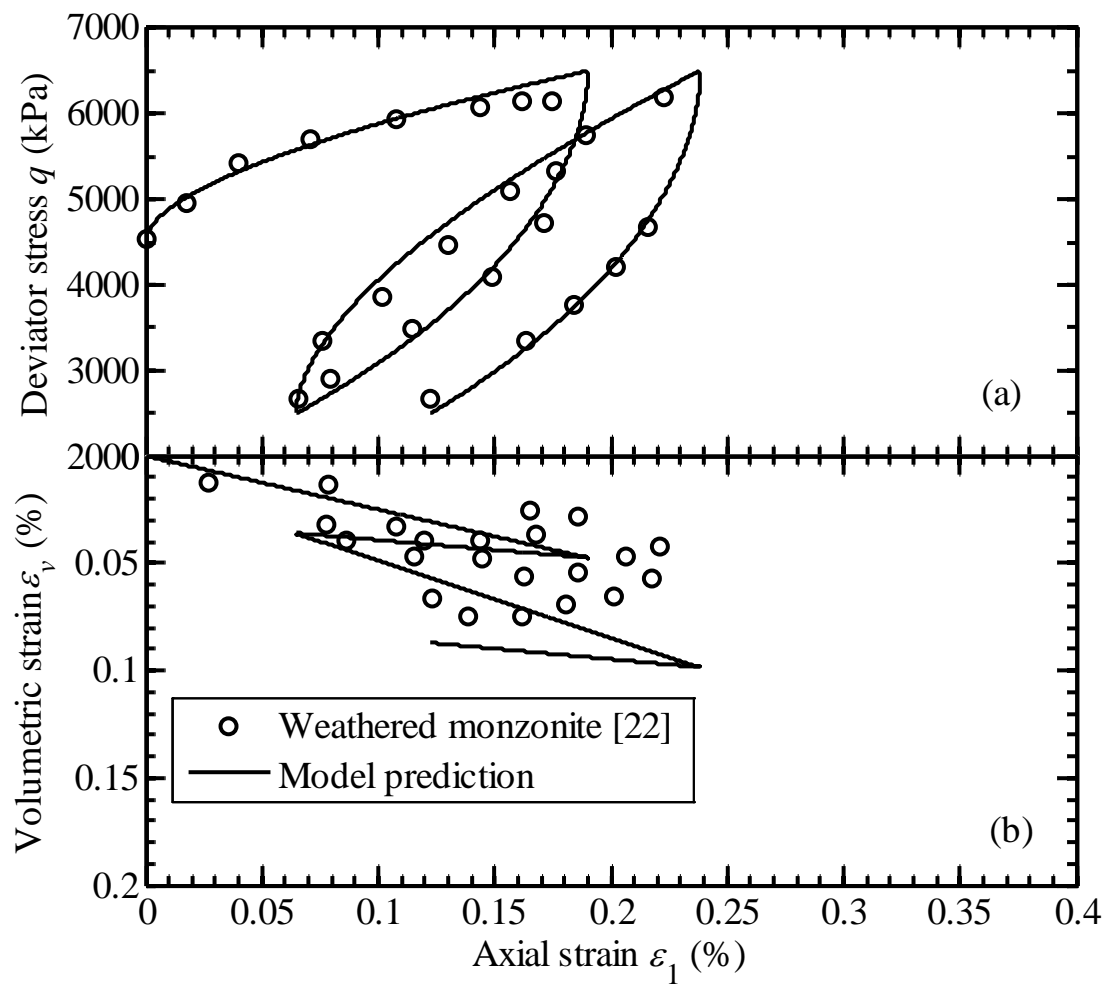


Fig. 10. Representation of the stress strain behaviour of weathered monzonite [22]